Article

Not peer-reviewed version

Integrated Whole-Transcriptome Analysis to Elucidate the Core Regulatory Network of circRNA Involved in Ovarian Development and Reproductive Capacity Differences in Sheep: circRNA2058-miR-9226-5p-MET Axis

Bo Gu , Anqi Wang , Xinmiao Yu , Ying Li , Yao Cong , Huaizhi Jiang *

Posted Date: 3 September 2025

doi: 10.20944/preprints202509.0351.v1

Keywords: Ujumqin sheep; Small-tailed Han sheep; circRNA-miRNA-mRNA; ovary

 doi:10.20944/preprints202509.0351.v1

Article

Integrated Whole-Transcriptome Analysis to Elucidate the Core Regulatory Network of circRNA Involved in Ovarian Development and Reproductive Capacity Differences in Sheep: circRNA2058-miR-9226-5p-MET Axis

Bo Gu [1], Anqi Wang [2], Xinmiao Yu [1], Ying Li [1], Yao Cong [1] and Huaizhi Jiang [2,*]

[1] College of Life Science, Jilin Normal University, Siping 136000, China

[2] College of Animal Science and Technology, Jinlin Agricultural University, Changchun 130118, China

* Correspondence: jianghz6806@126.com; Tel: 13756293858

Simple Summary

This study investigated the genetic regulation of ovarian development in sheep with high and low fecundity. Using whole-transcriptome sequencing of ovaries from different breeds and developmental stages, the researchers constructed competing endogenous RNA (ceRNA) networks. These networks revealed key interactions between circRNAs, miRNAs, and mRNAs. A central regulatory axis, circRNA2058-miR-9226-5p-*MET*, was identified and experimentally validated. This axis acts as a critical molecular switch controlling follicular development. The findings provide important insights into the molecular mechanisms behind sheep reproduction and offer a foundation for developing new strategies to improve reproductive efficiency in sheep.

Abstract

(1) Background: This study aims to systematically identify key candidate genes and the regulatory networks governing ovarian development in sheep breeds with divergent fecundity. Focusing on elucidating the central regulatory roles of these factors during distinct ovarian developmental stages in highly prolific breeds, the research seeks to reveal the mechanism by which multilevel regulatory networks synergistically determine ewe reproductive capacity. (2) Methods: This study utilized the ovaries from the low-fertility sheep breed Ujumqin sheep, the high-fertility sheep breed Small-tailed Han sheep, and various developmental stages of Small-tailed Han sheep as research subjects. Through whole-transcriptome sequencing analysis, differentially expressed mRNAs(DEGs) and non-coding RNAs (ncRNAs) were screened, and a ceRNA regulatory network was constructed and subjected to bioinformatic analysis. The dual-luciferase reporter gene detection system was employed to validate the targeting relationships within the obtained key circRNA-miRNA-mRNA networks. Finally, qRT-PCR was used to verify the accuracy of the sequencing results. (3) Results: The results revealed that the different fecundity groups constructed a ceRNA network comprising 116 differentially expressed circRNAs (DECs), 46 differentially expressed miRNAs (DEMs), and 82 DEGs. Similarly, the groups representing different ovarian developmental stages constructed a ceRNA network consisting of 186 DECs, 143 DEMs, and 338 DEGs. Functional enrichment analysis identified several reproduction-related signaling pathways, such as the MAPK, JAK-STAT, and WNT signaling pathways (in the different fecundity groups), and the MAPK, Ras, WNT, and Hippo signaling pathways (in the different ovarian developmental stage groups). Through comprehensive analysis of the reproduction-related pathways and screening of genes co-regulating the ceRNA networks in both comparison groups, a circRNA-miRNA-mRNA regulatory network was constructed. This analysis ultimately identified circRNA2058-miR-9226-5p-*MET* as playing a core regulatory role. The targeting relationship was validated using the dual-luciferase reporter assay system. The results demonstrated that miR-9226-5p mediates the expression of *MET* through

 doi:10.20944/preprints202509.0351.v1

sponging by circRNA2058. The accuracy of the sequencing results was further confirmed by qRT-PCR analysis of 8 randomly selected circRNAs and 8 miRNAs. (4) Conclusions: This study innovatively deciphered the synergistic regulatory network involving DE ncRNAs and their target genes. We identified, for the first time, a pivotal ceRNA regulatory axis: circRNA2058-miR-9226-5p-*MET*, which functions as a critical molecular switch driving the follicular dominance process in sheep. This discovery establishes a molecular foundation for precisely targeting core regulators of ovine reproductive efficiency, deepens our understanding of the core regulatory mechanisms governing sheep reproductive biology, and offers significant guidance for innovating strategies to enhance sheep reproductive efficiency.

Keywords: Ujumqin sheep; Small-tailed Han sheep; circRNA-miRNA-mRNA; ovary

1. Introduction

Since the 1980s, market demand for mutton sheep has steadily increased, making the mutton sheep industry a key focus in the development of China's sheep husbandry. To enhance the reproductive performance of sheep populations, China has prioritized the establishment of robust breeding systems, integrating both traditional and modern breeding techniques to develop and select new breeds. The Small-tailed Han sheep, recognized for its year-round estrus and high prolificacy, is frequently utilized as a maternal breed. However, despite China's rich diversity of sheep genetic resources, high-fertility breeds remain scarce. The overwhelming majority of sheep breeds exhibit low fertility. The Ujumqin sheep, a representative low-fertility breed, is renowned as "one of the breeds producing the highest quality meat among livestock" in its region. Its dairy products, meat, and wool are all of superior quality. Nevertheless, its application is significantly constrained by reproductive characteristics such as a long breeding cycle, low reproductive rate, and seasonal breeding patterns. Consequently, employing breeding strategies to improve the reproductive efficiency of low-fertility populations has become a strategic priority.

The ovary, as the central organ of the ewe reproductive system, exhibits a structure and functional status closely linked to fertility. Consequently, research into the reproductive regulatory functions of the ovary has consistently been a focal and challenging area in sheep husbandry. The advent of second-generation high-throughput parallel sequencing (Next-generation sequencing, NGS) technologies within molecular breeding has enabled transcriptome analyses based on RNA sequencing (RNA-seq). These analyses have revealed that the ovary harbors a complex transcriptional network, encompassing both coding and non-coding genes, which closely regulates key reproductive traits in sheep. This approach provides a crucial technical platform and research perspective for advancing our understanding of the molecular mechanisms through which the ovary modulates ovine reproductive performance. During a comparative analysis of ovarian follicles in Boer goats and Macheng black goats, researchers identified 37 DECs between the two breeds. This finding indicates that circRNA expression levels may significantly influence ovarian follicle development, which may ultimately lead to the observed differences in their reproductive rates[1]. During an in-depth analysis of Xiang pig ovarian samples collected during the estrus and diestrus stages, 156 DECs were identified. They proposed that these DECs may regulate gene expression during the porcine estrous cycle. Additionally, host genes of these DECs were predicted, revealing 432 miRNA targets. It was noted that each circRNA could contain one or more miRNA binding sites[2]. Previous research demonstrated that in bovine oocytes, ciRS-187 may upregulate BMPR2 expression by suppressing miR-187[3]. Similarly, a novel circRNA, circSLC41A1, was found to enhance SRSF1 expression through competitive binding with miR-9820-5p, thereby regulating apoptosis in porcine follicular granulosa cells[4]. The study revealed that chi_circ_0031209 and chi_circ_0019448 play critical roles in reproduction during the luteal phase by modulating prolactin receptor expression in both high- and low-yield goats. Conversely, chi_circ_0014542 is involved in regulating *WNT5A* expression during the follicular phase, thereby modulating follicular

 doi:10.20944/preprints202509.0351.v1

development in mammals[5]. Comprehensive transcriptome sequencing of ovaries from sheep with divergent fertility revealed 180 DECs. We further demonstrated that novel_circ_0041512 modulates ovarian development in sheep by sponging miR-125b[6]. Previous research identified five key ceRNA interaction networks that regulate goat reproductive performance. Further analysis showed that these networks primarily influence ovarian function and reproductive performance by regulating biological processes such as germ cell development and oocyte development[7].

In summary, this study utilized ovarian tissues from the low-prolificacy breed Ujumqin sheep (Ud group), the high-prolificacy breed Small-tailed Han sheep (Sad group), and Small-tailed Han sheep at different developmental stages (Som group-juvenile, Stm group-pre-pubertal, Sad group-sexually mature) as research subjects. With three biological replicates per group, we performed whole-transcriptome sequencing and subsequent bioinformatic analyses. The primary objectives were to identify key candidate genes and regulatory networks capable of concurrently modulating both breed-specific fecundity differences and developmental stage-dependent reproductive capacity in sheep. This research aims to elucidate the underlying multi-dimensional regulation mechanisms governing ovine reproductive efficiency. Furthermore, the findings are expected to provide a theoretical foundation and valuable references for improving reproductive performance in low-prolificacy sheep breeds and enhancing overall ewe fertility through targeted breeding programs.

2. Materials and Methods

2.1. Sample Collection

Ovarian tissues were collected from Small-tailed Han sheep and Ujumqin sheep reared at Guofeng Livestock Breeding Farm (Songyuan, Jilin Province). Three healthy one-month-old lambs, six-month-old lambs, and three adult multiparous Small-tailed Han sheep ewes—all under identical feeding conditions—were selected, along with three adult multiparous Ujumqin sheep ewes. Following slaughter, ovarian tissue blocks (3–5cm^2) were excised and immediately flash-frozen in liquid nitrogen for subsequent experiments.

2.2. Total RNA Extraction and Library Construction

Total RNA was extracted from ovarian tissues using TRIzol reagent, and its concentration and integrity were assessed using the NanoDrop2000 spectrophotometer and the Agilent Bioanalyzer. Strand-specific libraries(fr-firstrand) were constructed using the ribosomal RNA (rRNA) depletion method. After passing quality inspection, high-throughput sequencing was performed on the Illumina NovaSeqTM 6000 platform. Sequencing was conducted in paired-end mode with a read length of 150 bp (PE150), enabling simultaneous detection of both mRNA and circRNA expression levels. For miRNA analysis, small RNA (sRNA) sequencing libraries were prepared using the TruSeqTM Small RNA Sample Prep Kit (Illumina, San Diego, USA). After library qualification, sequencing was carried out on the Illumina HiSeq 2000/2500 platform, generating single-end 50 bp reads (SE50).

2.3. Sequencing Data Quality Control and Analysis

Raw sequencing data were processed using Cutadapt[8] to remove adapter sequences and low-quality reads, yielding high-quality clean data. Clean reads were then aligned to the reference genome using HISAT2[9–11]. Gene-level read counts were quantified based on genomic coordinates defined in the genome annotation file. Using the alignment results, transcript reconstruction was conducted with StringTie[11–13], and the expression levels of all identified genes in each sample were subsequently quantified.

circRNA analysis diverges from mRNA analysis by focusing on reads that discordantly map to the reference genome. Reads failing to align linearly were analyzed to detect back-splice junctions

 doi:10.20944/preprints202509.0351.v1

(BSJs). circRNAs were identified using the intersection of predictions from both CIRCexplorer2[14] and CIRI[15].

miRNA processing was performed using ACGT101-miR (v4.2). The pipeline included: 3'adapter trimming, removal of low-complexity sequences, and size selection (retaining reads 18-26 nt in length). Filtered reads were sequentially aligned against multiple RNA databases (including mRNA, RFam, and Repbase) to remove non-miRNA sequences. Final miRNA identification was achieved by mapping reads to precursor miRNAs and the reference genome.

2.4. Differential Expression Analysis and Target Gene Prediction

For the identification and quantification of circRNAs, we relied on back-splice junction (BSJ) reads. Differential expression analysis of circRNAs between groups was performed using edgeR, with circRNAs satisfying $|\log_2 fc| \geq 1$ and $P < 0.05$ considered significantly differentially expressed. Given the inherent variation in circRNA expression across different tissues and developmental stages, we annotated the circRNAs based on their genomic locations and their associations with genes. Functional annotation of the circRNAs was primarily derived from the known functions of their parental genes.

For miRNAs, those with $P < 0.05$ were deemed differentially expressed. Target genes of these significantly differentially expressed miRNAs were predicted by intersecting the results from TargetScan (v5.0) and miRanda (v3.3a), applying stringent thresholds (TargetScan_score ≥ 50 and miRanda_Energy < -10).

2.5. Construction and Bioinformatics Analysis of the ceRNA Network

A crucial function of circRNAs is their ability to act as molecular sponges that sequester miRNAs. This competitive binding disrupts the regulatory activity of miRNAs on their target genes, ultimately altering protein expression levels. Within the ceRNA regulatory network, miRNAs occupy a central position. To construct the competing circRNA-miRNA-mRNA regulatory triplets, we calculated Pearson correlation coefficients (r). Pairs exhibiting a significant negative correlation ($r < -0.4$ and $P < 0.05$) for both circRNA-miRNA and miRNA-mRNA interactions were selected. This identified triple network was then visualized using Cytoscape software.

Furthermore, target genes within this regulatory network were subjected to functional annotation and signaling pathway analysis utilizing the Gene Ontology (GO) database (http://geneontology.org/) and the Kyoto Encyclopedia of Genes and Genomes (KEGG) database (http://www.genome.jp/kegg/).

2.6. qRT-PCR and Sanger Verification

To validate the accuracy of the RNA-seq results, four circRNAs and four miRNAs were randomly selected from each comparison group and subjected to qRT-PCR validation, with primer sequences detailed in Supplementary Table S1. Relative quantification was performed using the $2^{-\Delta\Delta Ct}$ method, followed by one-way ANOVA and significance testing using SPSS 18.0.

To further confirm the circularity of the designed circRNA primers, PCR amplification was performed for all eight circRNAs using both cDNA and gDNA templates. The resulting products were analyzed by 1.5% agarose gel electrophoresis to validate their circular characteristics.

2.7. Dual-Luciferase Reporter Assay

Prediction of binding sites was performed using the RNAhybrid software based on ncRNA sequence information, followed by dual-luciferase reporter assay for verification.

2.8. Recombinant Plasmids Preparation

Based on predicted interaction regions, mutant and wild-type sequences were designed and directionally cloned into the pCHECK2 plasmid backbone.

 doi:10.20944/preprints202509.0351.v1

2.9. Cell Transfection

HEK293T cells were thawed and cultured in 25 cm^2 flasks at 37 ℃. Upon reaching 90% confluence, cells were trypsinized and seeded at equal density into 96-well plates. Triplicate biological replicates were prepared. Co-transfection was performed according to experimental groupings, with transfection completed the following day.

2.10. Reporter Signal Measurement

Plates were equilibrated at room temperature for 30 min. Luciferase Assay Reagent I (equal to culture medium volume) was added to each well, followed by gentle pipetting. After 10 min incubation, luminescence signals were measured using a microplate reader.

2.11. Normalization Control Measurement

An equal volume of Stop & Glo® Reagent was added to each well. Following gentle mixing and 10 min incubation at room temperature, renilla signals were recorded using the same instrument.

2.12. Data Normalization

Firefly/renilla luminescence ratios were calculated for each sample. Data were analyzed using appropriate statistical methods.

3. Results

3.1. Sequencing Data Analysis

Ovarian tissues were collected from twelve samples: three one-month-old Small-tailed Han sheep(Som1, Som2, Som3), three six-month-old Small-tailed Han sheep(Stm1, Stm2, Stm3), three adult multiparous Small-tailed Han ewes(Sad1, Sad2, Sad3), and three adult multiparous Ujimqin sheep ewes(Ud1, Ud2, Ud3). Total RNA from all samples passed quality control, with both concentration and integrity meeting the requirements for sequencing, as detailed in Supplementary Table S2. Following sequencing, raw reads were filtered; the resulting data are presented in Tables 1 and 2. For both mRNA and circRNA sequencing, over 98.5% of bases achieved a Q20 score and over 95% achieved a Q30 score in each sample. The GC content ranged from 45% to 50.5%. Similarly, for sRNA sequencing, Q20 and Q30 scores exceeded 95% in all samples, with GC content between 50.62% and 51.98%. These results demonstrate high-quality sequencing data with qualified quality control metrics, confirming their suitability for subsequent analyses.

Table 1. mRNA and circRNA sequencing data production quality.

Sample	Raw Data	Valid Data	Mapped reads/%	Q20%	Q30%	GC content/%
Som_1	95,584,162	92,544,232	87,671,478(94.73%)	99.97	97.81	45.00
Som_2	93,194,002	90,150,580	85,397,972(94.73%)	99.97	97.84	44.00
Som_3	93,566,726	90,707,218	84,656,216(93.33%)	99.96	97.58	45.00
Stm_1	93,780,650	90,919,404	86,062,585(94.66%)	99.97	97.78	45.00
Stm_2	91,917,068	88,670,432	82,933,703(93.53%)	99.98	98.30	49.00
Stm_3	71,302,642	67,362,198	60,153,911(89.30%)	98.50	94.59	45.00
Sad_1	94,092,386	91,107,390	86,158,306(94.57%)	99.96	97.78	45.00
Sad_2	97,790,686	94,803,474	89,533,252(94.44%)	99.96	97.71	45.00
Sad_3	89,825,602	86,701,034	80,875,819(93.28%)	99.97	98.16	48.50
Ud_1	73,320,580	70,898,902	65,359,324(92.19%)	99.85	97.83	47.00
Ud_2	92,249,184	87,955,300	82,065,791(93.30%)	99.77	97.86	50.50
Ud_3	71,516,612	68,959,698	63,802,517(92.52%)	99.81	97.60	48.00

 doi:10.20944/preprints202509.0351.v1

Table 2. sRNA sequencing data production quality.

Sample	Raw Data	Valid Data	Mapped reads/%	Q20%	Q30%	GC content/%
Som_1	13,916,096	9,366,661	9,257,071(98.83%)	97.91	96.89	51.78
Som_2	12,153,463	7,973,465	7,861,836,(98.60%)	97.67	96.68	51.60
Som_3	15,083,990	9,398,231	9,259,137(98.52%)	97.02	95.67	51.78
Stm_1	9,076,908	5,229,613	5,161,628(98.70%)	97.74	96.52	51.98
Stm_2	8,729,542	7,235,145	7,180,158(99.24%)	97.63	96.44	51.03
Stm_3	10,569,235	5,463,213	5,393,284(98.72%)	97.35	96.04	50.62
Sad_1	10,567,624	6,971,109,	6,898,609,(98.96%)	97.92	96.91	51.40
Sad_2	9,796,916	7,951,578	7,863,315(98.89%)	97.92	96.96	51.22
Sad_3	10,036,758	6,868,427	6,794,248,(98.92%)	97.29	96.07	51.11
Ud_1	11,079,361	6,789,313	6,743,146(99.32%)	99.24	97.13	51.14
Ud_2	11,405,958	7,210,142	7,160,392(99.31%)	99.26	97.10	50.87
Ud_3	11,156,801	7,387,622	7,321,133(99.10%)	99.28	97.18	50.94

3.2. Screening and Identification of circRNAs and miRNAs

CircRNA identification results revealed that 4587, 3860, 4332, 3167, 6729, 2989, 7025, 6533, 7645, 8564, 11248, and 8435 circRNAs were detected in the 12 samples (Som1, Som2, Som3, Stm1, Stm2, Stm3, Sad1, Sad2, Sad3, Ud1, Ud2, Ud3), respectively. Further analysis of the genomic origins of the identified circRNAs demonstrated that exonic circRNAs constituted the predominant category, followed by intronic ciRNAs and intergeniccircRNAs (Figure 1a). The length of the identified circRNAs primarily ranged between 200 and 20,000 nucleotides (nt) (Figure 1b), and the majority were formed by the circularization of 2 to 4 exons (Figure 1c). Following normalization, the transcript expression levels of circRNAs were comparable across the different groups (Figure 1d).

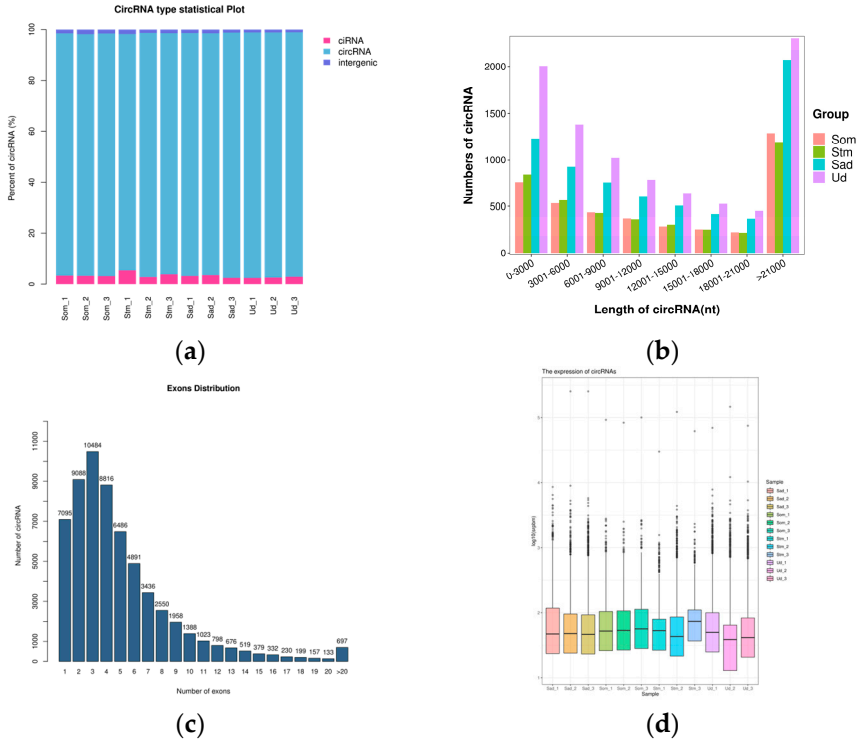

Figure 1. General Characteristics of circRNAs. (**a**): circRNA type statistics; (**b**): circRNA sequence length; (**c**): circRNA Exon Count Distribution; (**d**): circRNA expression distribution map.

The miRNA annotation results revealed that novel miRNAs constituted the largest proportion, followed by known miRNAs and mRNAs. The proportions of all other types were nearly negligible(Figure 2a). The percentage of total rRNA serves as an indicator of sample quality. High-quality animal samples typically exhibit total rRNA content constituting less than 40%[16]. In this

 doi:10.20944/preprints202509.0351.v1

study, the total rRNA content in all four ovarian libraries was close to 0%, indicating exceptionally high sample quality. Furthermore, analysis of the first nucleotide preference for the identified miRNAs demonstrated that both known and predicted miRNAs exhibited a marked preference for uracil (U) at their 5' termini (Figure 2b). The length distribution of miRNAs was highly consistent across all libraries, ranging predominantly from 20 to 24 nt. The most abundant miRNAs were 22 nt in length, consistent with typical miRNA sizes (Figure 2c).

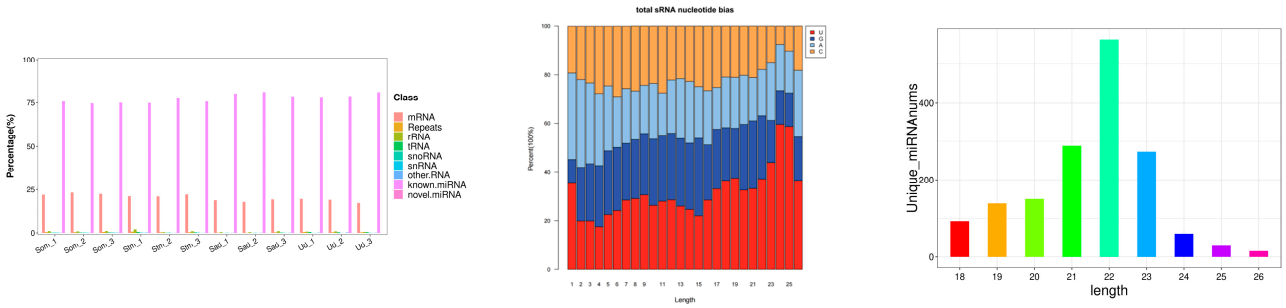

(**a**) (**b**) (**c**)

Figure 2. General characteristics of miRNA. (**a**): Categories of identified ncRNAs via sequencing in Som、Stm、Sad and Ud groups; (**b**): Bias distribution of the first base of miRNA sequence; (**c**): Length distribution of clean reads from identified miRNA fragments.

3.3. Differential Expression Analysis

In the differential expression analysis of circRNAs, we identified a total of 517 DECs between the different fertility groups (Sad vs. Ud), comprising 408 up-regulated and 109 down-regulated circRNAs (Figure 3a). For comparisons between different ovarian developmental stages: the Som vs. Stm comparison yielded 161 DECs (77 up-regulated, 84 down-regulated); Stm vs. Sad yielded 232 DECs (50 up-regulated, 182 down-regulated); and Som vs. Sad yielded 282 DECs (53 up-regulated, 229 down-regulated) (Figure 3b).

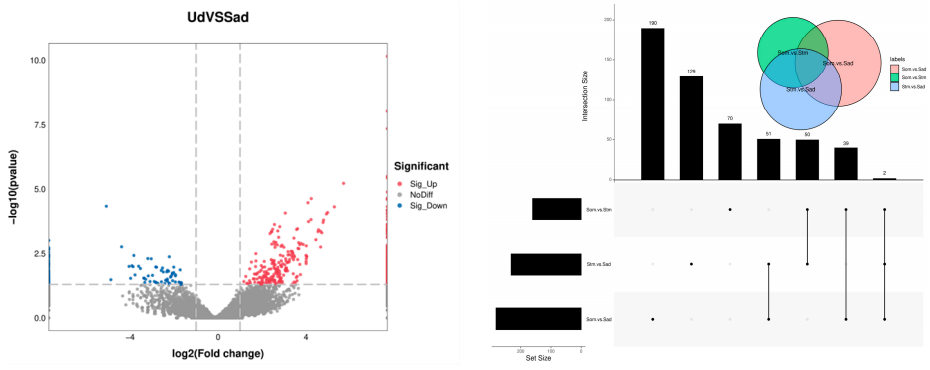

(**a**) (**b**)

Figure 3. Volcano plot and Venn diagram of differentially expressed circRNAs. (**a**): different fecundity groups; (**b**): different ovarian developmental stages.

To elucidate the relationships among DECs in different comparison groups, protein-protein interaction (PPI) networks were constructed for both up- and down-regulated host genes using interactions with a Confidence score ≥ 0.40. The results are presented in Figure 4. Analysis of the protein interactions within these networks revealed the following: In the up-regulated host gene network: The 102 up-regulated genes formed 113 interaction pairs. Hub genes identified within this network included *EXOC6B*, *SUPT3H*, *USP3*, *PDS5B*, and *NCOA6*. In the down-regulated host gene network: The 15 down-regulated genes formed 12 interaction pairs. Hub genes in this network were *VPS13B*, *PDS5B*, and *USP3*. Notably, *USP3* emerged as a common hub gene shared between

 doi:10.20944/preprints202509.0351.v1

both networks. It exhibited significant interactions with several key nodes, including *PDS5B*, *CEP*120, *CEP*70, *KAT2B*, *FBXL*17, and *SUPT3H*. This suggests that *USP*3 may play a critical role and potentially influence female germ cell development.

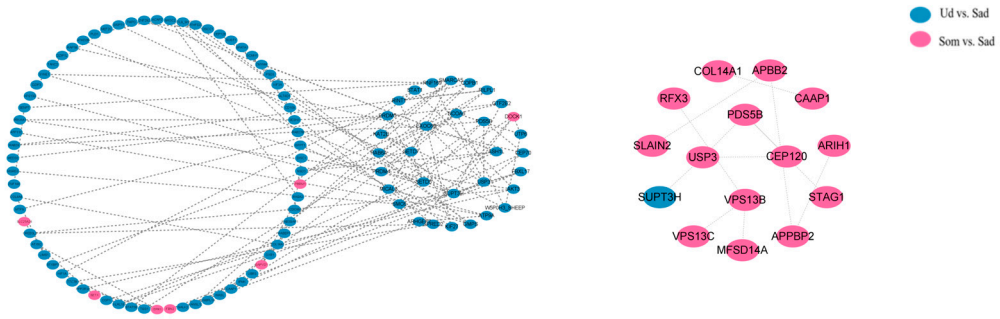

(**a**) (**b**)

Figure 4. PPI analysis of DE circRNA host gene. (**a**):Up-regulated of host gene; (**b**):Down-regulated of host gene.

In the screening analysis for DEMs, 103 DEMs were identified between the different fecundity comparison groups (Sad vs. Ud), comprising 40 up-regulated and 63 down-regulated miRNAs, as illustrated in Figure 5a. Comparative analysis of different ovarian developmental stages revealed 227 DEMs between the Som vs. Stm groups (170 up-regulated, 57 down-regulated), 43 DEMs between the Stm vs. Sad groups (22 up-regulated, 21 down-regulated), and 330 DEMs between the Som vs. Sad groups (279 up-regulated, 51 down-regulated), shown in Figure 5b.

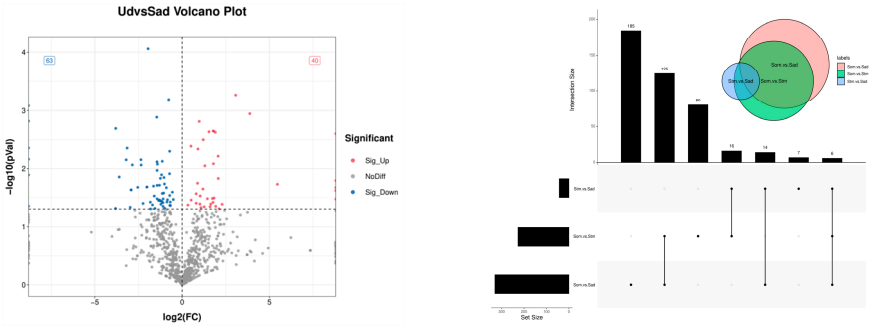

(**a**) (**b**)

Figure 5. Volcano plot and Venn diagram of differentially expressed miRNAs. (**a**): different fecundity groups; (**b**): different ovarian developmental stages.

To elucidate the regulatory role of miRNAs in female sheep reproduction, we removed novel genes and screened for reproduction-associated DEMs and DEGs from each comparative group. Subsequently, miRNA-mRNA regulatory networks were constructed to explore interactions between candidate DEMs and their target DEGs in ovarian function. Following comparisons between fertility groups, we identified and constructed a focused DEM-DEG regulatory network comprising 3 known DEMs (miR-214, miR-320b, miR-9226-5p) and 143 DEGs (Figure 6a). Similarly, analysis of ovarian developmental stages revealed a compact ceRNA network involving 3 known miRNAs (miR-9226-5p, miR-27b-3p, miR-4286) and 344 DEGs (Figure 6b).

 doi:10.20944/preprints202509.0351.v1

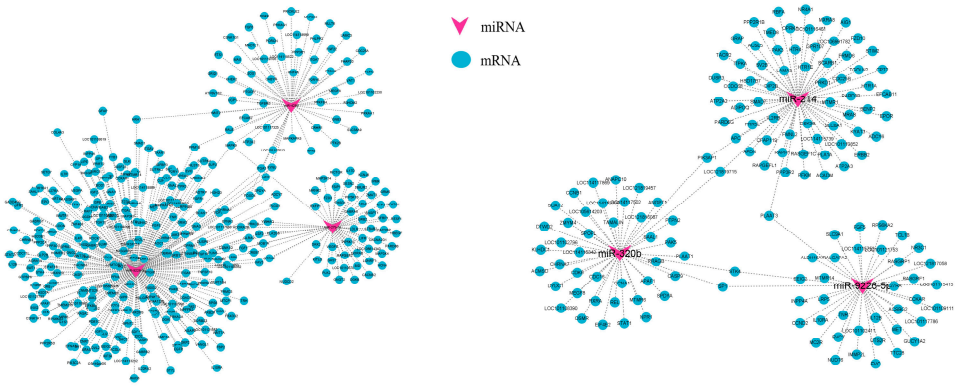

(**a**) (**b**)

Figure 6. Overview of miRNA and target genes networks. (**a**): The DEM-DEG interaction network in the Ud vs. Sad group; (**b**): The DEM-DEG interaction network in the Som vs. Stm vs. Sad group.

3.4. ceRNA Network Analysis

Focusing on DEMs, we integrated DECs acting as miRNA sponges and DEGs targeted by DEMs. DEMs were identified from the intersection of two comparative groups, and a regulatory network was constructed. Due to the excessively large network size, core genes were selected as the intersection of the top 10 miRNAs with the highest interaction probability across relationship pairs. This approach yielded two concise ceRNA networks relevant to our study, as illustrated in Figure 7. The ceRNA network derived from the comparison of different fecundity groups (Ud vs. Sad) comprised 116 DECs, 46 DEMs, and 82 DEGs (Figure 7a). The network obtained from comparing different ovarian developmental stages (Som vs. Stm vs. Sad) consisted of 186 DECs, 143 DEMs, and 338 DEGs, forming a circRNA-miRNA-mRNA regulatory network (Figure 7b).

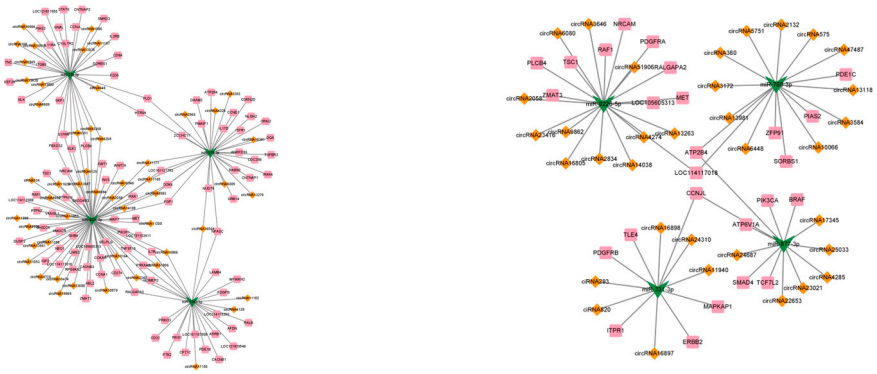

(**a**) (**b**)

Figure 7. ceRNA Regulatory Network. (**a**): different fecundity groups; (**b**): different ovarian developmental stages.

Further GO and KEGG enrichment analyses were performed on the target genes within the ceRNA regulatory network. In the comparison groups of sheep with differing fecundity, several biological processes and pathways related to reproduction were significantly enriched (Figure 8a), including the MAPK signaling pathway, JAK-STAT signaling pathway, and WNT signaling pathway. In the comparison groups of different developmental stages, genes such as *PAK*1, *KIT*, *FGF*9, and *PRKCG* were found to be concurrently involved in both the MAPK signaling pathway and the Ras signaling pathway. Additionally, genes including *WNT*3, *WNT*16, *WNT*2, and *FZD*3 participated simultaneously in both the WNT signaling pathway and the Hippo signaling

 doi:10.20944/preprints202509.0351.v1

pathway (Figure 8b). These genes represent potential candidate genes implicated in reproductive processes.

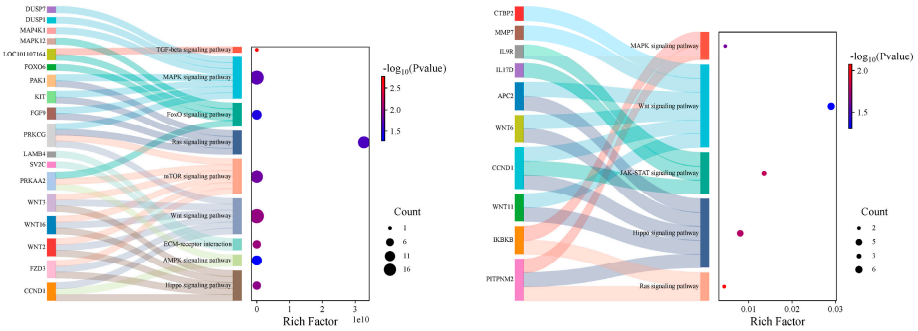

(**a**) (**b**)

Figure 8. Bubble Map of Target Gene KEGG-Enriched Sankey. (**a**): different fecundity groups; (**b**): different ovarian developmental stages.

Taken together, we constructed a circRNA-miRNA-mRNA regulatory network (Figure 9) by selecting genes functionally associated with reproduction that were co-regulated in the ceRNA networks of both comparison groups. This network comprised 4 miRNAs, 6 circRNAs, and 12 mRNAs, forming 22 interaction pairs. Functional analysis implicated the *MET* gene in ovarian development and follicular dominance. Consequently, the circRNA2058-miR-9226-3p-*MET* axis was selected for validation using a dual-luciferase reporter assay to confirm the predicted targeting relationships.

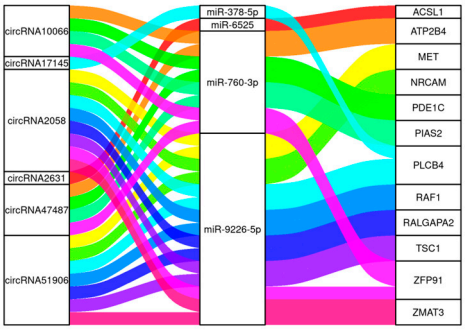

Figure 9. ceRNA Network Sankey Diagram.

3.5. qRT-PCR and Sanger Verification

Validation of eight selected circRNAs by qRT-PCR is presented in Figure 10. The expression trends observed in both RNA-seq and qRT-PCR analyses were consistent, indicating the reliability of the RNA-seq results. Validation of the designed circRNA primers demonstrated their specificity: amplification using cDNA templates yielded bands of the expected size, while no bands were produced with genomic DNA (gDNA) templates (Supplementary Figure S1). Sanger sequencing of the cDNA-derived amplicons confirmed that the sequences spanning the back-splice junctions matched the circRNA sequencing data, verifying the circular nature of these transcripts (Supplementary Figure S1).

 doi:10.20944/preprints202509.0351.v1

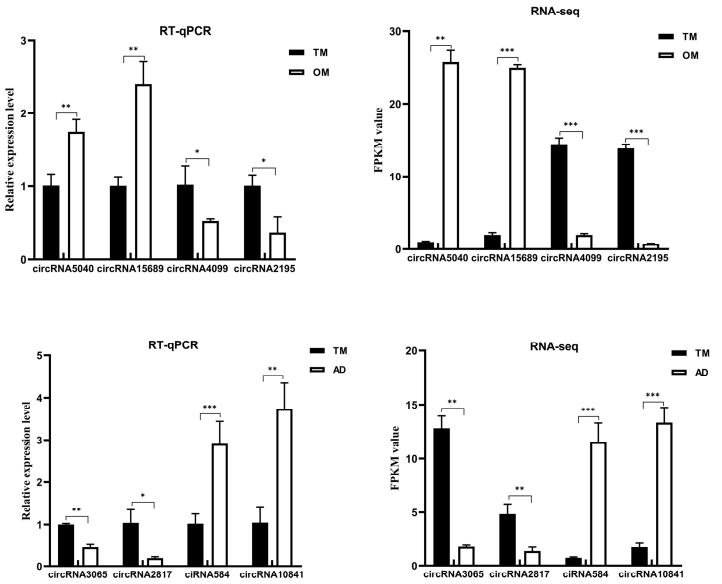

Figure 10. qRT-PCR validation of the RNA-Seq data for circRNAs.

The relative quantification results of eight randomly selected miRNAs from the two comparison groups are shown in Figure 11. Their expression levels agreed with the RNA-seq data, further demonstrating the accuracy and reproducibility of the RNA-seq results.

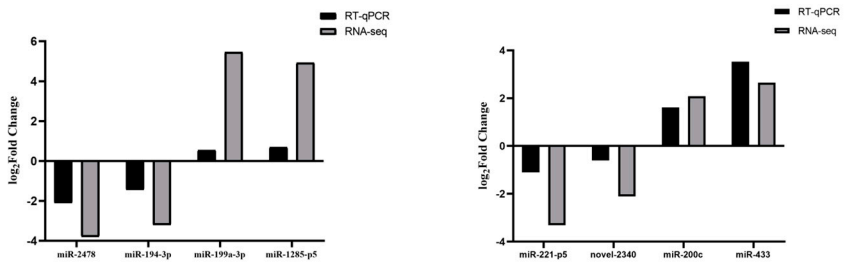

Figure 11. qRT-PCR validation of the RNA-Seq data for miRNAs.

3.6. Dual-Luciferase Reporter Assay

As depicted in Figure 12a, the base pairing occurs between the 3'UTR region of the *MET* gene and miR-9226-5p. Luciferase reporter assays (Figure 12b) demonstrated that miR-9226-5p significantly suppressed the luciferase activity of *MET*-F compared to the NC control group ($P < 0.05$), indicating specific binding between them. Following site-directed mutagenesis, this regulatory effect was abolished, as evidenced by the lack of a statistically significant difference ($P > 0.05$) in luciferase activity for the mutant construct MET-T, confirming successful mutant construction. The binding site within the 3'UTR region of circRNA2058 (Figure 12c) for miR-9226-5p was further validated by luciferase assays (Figure 12d). Transfection with miR-9226-5p significantly reduced the reporter activity of circRNA2058-F ($P < 0.05$), whereas the luciferase intensity of the mutant circRNA2058-T remained stable ($P > 0.05$). These results successfully confirm the interaction between this circular RNA and the miRNA.

 doi:10.20944/preprints202509.0351.v1

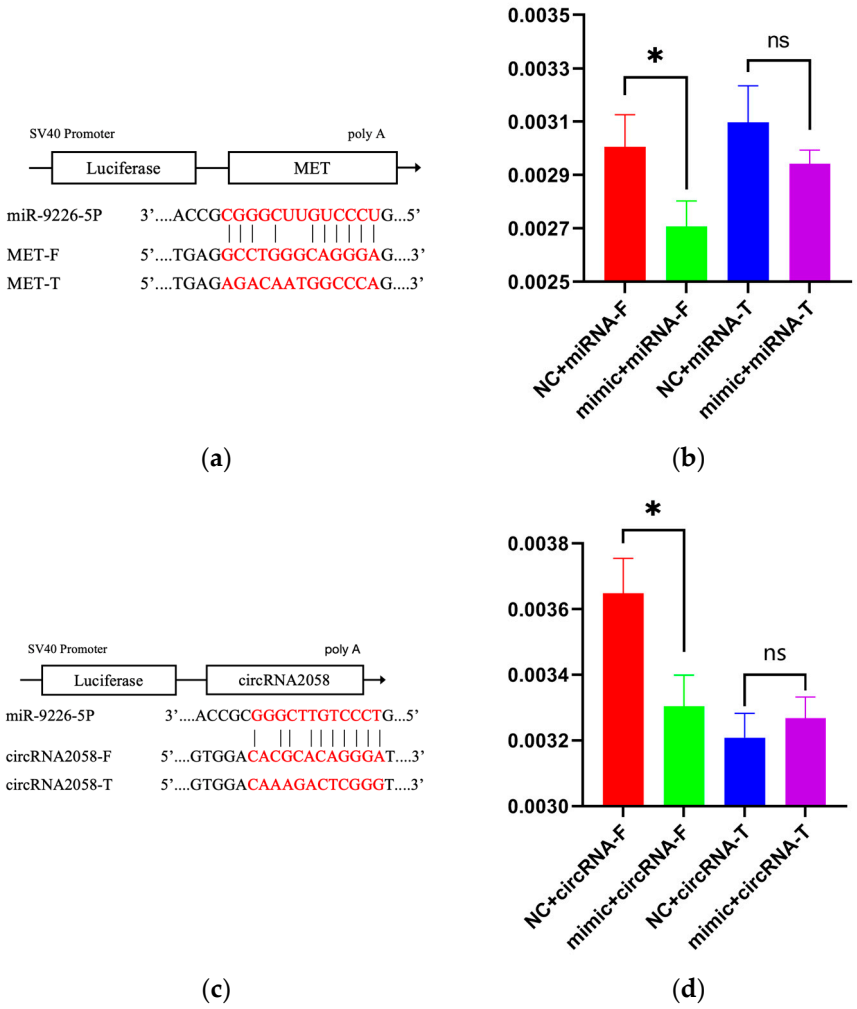

Figure 12. Targeting Relationship Validation. (**a**): Complementary nucleotide sequence of *MET*-3'UTR and miR-9226-5p; (**b**): *MET* and miR-9226-5p double luciferase report results; (**c**): Complementary nucleotide sequence of circRNA2058-3'UTR and miR-9226-5p; (**d**):circRNA2058 and miR-9226-5p double luciferase report results.

4. Discussion

Elucidating the genetic basis of prolificacy traits is critical for molecular breeding in sheep. The ovarian microenvironment, a central regulatory hub within the female reproductive axis, critically governs follicular development dynamics and ovulation rates in mammals, thereby profoundly influencing reproductive success. Consequently, ovarian tissue serves as a primary sequencing target for identifying key functional genes associated with multiple lambing and high fecundity. Emerging research highlights ncRNAs as pivotal regulators within ovarian gene networks, offering significant theoretical insights into ovine reproductive mechanisms. Among these, circRNAs exhibit exceptional intracellular stability and resistance to degradation due to their closed-loop structure. Functioning as efficient molecular sponges, circRNAs sequester miRNAs to derepress their target mRNAs, establishing ceRNA networks. Existing studies confirm that ceRNA networks play crucial roles in mammalian reproductive hormone synthesis, follicular maturation/atresia, and early embryonic development regulation[17–19]. Therefore, elucidating the expression dynamics and functional roles of ceRNA networks in sheep ovaries—across varying fertility phenotypes and developmental stages—holds substantial biological significance for deciphering the regulatory mechanisms underlying ovine reproductive performance.

This study employed RNA-Seq technology coupled with differential expression analysis to profile mRNA and ncRNA expression in groups differing in fecundity and at various ovarian developmental stages. Subsequent construction of a ceRNA network and bioinformatic analyses

 doi:10.20944/preprints202509.0351.v1

identified several reproduction-associated signaling pathways. These include the MAPK, JAK-STAT, and WNT signaling pathways (in the fecundity comparison groups), and the MAPK, Ras, WNT, and Hippo signaling pathways (in the ovarian developmental stage groups). The Hippo signaling pathway primarily regulates organ size and contact inhibition[20,21]. Within the ovary, its inhibited state may indirectly enhance ovulation rates by promoting primordial follicle activation[22] and granulosa cell proliferation[23]. This mechanism potentially contributes to variations in sheep fecundity. Studies indicate that all components of the Hippo pathway are expressed in the ovary, where it plays a critical role in regulating mammalian germ cell proliferation, follicular development, and corpus luteum formation[24]. The JAK-STAT signaling pathway is highly activated in dominant follicles, regulating granulosa cell proliferation and differentiation. JAK3 was found to interact with proteins such as LEPROTL1, INHBA, and CDKN1B, influencing granulosa cell viability by phosphorylating STAT family members, thereby determining follicular maturation or atresia[25]. The MAPK signaling pathway serves as a key messenger transmitting extracellular signals from the cell membrane to the nucleus[26]. It acts as a central molecular hub in regulating ovarian function, significantly influencing reproductive efficiency by coordinating follicular development, hormone synthesis, and cell fate determination[27,28]. The Ras signaling pathway is a key regulator of cell proliferation, differentiation, and apoptosis, and plays a critical role in the mammalian reproductive system. Its functions include regulating follicular development, oocyte maturation, steroid hormone synthesis, and ovulation[29,30]. The Wnt signaling pathway, a crucial pathway in reproduction, has been extensively investigated. Studies have demonstrated that miR-458b-5p regulates follicular development in the chicken ovary by targeting *CTNNB*1(β-catenin), a key gene within the Wnt signaling pathway[31]. Furthermore, microRNA-3061 was shown to induce premature ovarian insufficiency in mice by downregulating the expression of Wnt signaling pathway genes[32]. Additionally, research revealed that miR-29c targets *FZD*4, a Wnt pathway receptor, thereby inhibiting both Wnt signaling activation and granulosa cell (GC) apoptosis mediated by *SMAD*4-induced *FZD*4[33].

Comprehensive analysis of genes enriched in reproduction-related pathways identified *MET* as a common hub gene within the reproductive networks of both comparison groups, suggesting its critical role in reproductive regulation. The *MET* gene encodes the sole receptor for hepatocyte growth factor (HGF). Their specific binding interaction regulates gonadal development and germ cell proliferation[34]. Previous research has proposed *MET* as a key candidate gene influencing reproductive traits in Chinese Holstein cattle[35]. Furthermore, *MET* directly acts on vascular endothelial cells to modulate angiogenesis, enhance capillary density, and increase blood flow, thereby influencing injury repair and embryonic development[36,37]. During bovine follicular formation, Parrott's team demonstrated that *MET* in both theca and granulosa cells, in concert with estrogen and luteinizing hormone (LH), mediates granulosa cell proliferation by modulating the localized expression of HGF, thereby driving follicular maturation[38]. Collectively, these findings underscore the significant role of the *MET* gene in the genetic architecture of reproductive traits.

Comprehensive analysis of the constructed ceRNA network, validated using the dual-luciferase reporter assay system, ultimately confirmed that miR-9226-5p directly targets and regulates *MET* expression. Furthermore, circRNA2058 was demonstrated to function as a molecular sponge for miR-9226-5p. These findings collectively indicate that the circRNA2058-miR-9226-5p-*MET* ceRNA axis plays a potential regulatory role in the high fecundity trait of sheep. However, the precise mechanism remains unclear. Based on previous studies, we speculate that it may influence ovarian development by modulating granulosa cell proliferation and apoptosis, meriting further investigation.

5. Conclusions

This study employed transcriptome-wide co-analysis to construct a multi-dimensional ceRNA network implicated in the regulation of ovine ovarian development. From this network, we identified key candidate genes capable of concurrently modulating reproductive capacity across

 doi:10.20944/preprints202509.0351.v1

different sheep breeds and developmental stages. Particular focus was placed on the core regulatory axis comprising circRNA2058-miR-9226-5p-*MET*. The targeting relationships within this axis were validated using the dual-luciferase reporter assay system. These findings provide novel targets and a theoretical foundation for elucidating the genetic mechanisms underlying high fecundity in sheep, developing molecular breeding markers, and preventing reproductive disorders. Consequently, this work holds significant scientific and practical implications for enhancing ovine reproductive efficiency and advancing efficient breeding practices.

Supplementary Materials: The following supporting information can be downloaded at the website of this paper posted on Preprints.org, Figure S1: Verification of DECs; Table S1: Detection results of total RNA quality; Table S2: qRT-PCR primers sequence information.

Author Contributions: Conceptualization, B.G. and H.J.; methodology, B.G. and H.J.; validation, A.W.; formal analysis, B.G. and A.W.; investigation, X.Y. and Y.C.; resources, Y.L.; data curation, Y.L.; writing—original draft preparation, B.G.; writing—review and editing, B.G.; visualization, B.G.; supervision, X.Y.; project administration, B.G. and H.J.; funding acquisition, H.J.. All authors have read and agreed to the published version of the manuscript.

Funding: This research was supported by National Key Research and Development Program (2021YFF1000702).

Institutional Review Board Statement: All methods were carried out in accordance with relevant guidelines set by the Ministry of Agriculture of the People's Republic of China. All experimental protocols were approved by the Ethics Committee for Science and Technology of Jilin Normal University (KJLL20250403).

Informed Consent Statement: Not applicable.

Data Availability Statement: The raw RNA-seq data generated in this study have been deposited in the NCBI Sequence Read Archive (SRA) under the BioProject accession number PRJNA1289050.

Conflicts of Interest: The authors declare no conflicts of interest.

Abbreviations

The following abbreviations are used in this manuscript:

DECs	differentially expressed circRNAs
DEMs	differentially expressed miRNAs
DEGs	differentially expressed mRNAs
ncRNA	non-coding RNA
ceRNA	competing endogenous RNA
GO	Gene Ontology
KEGG	Kyoto Encyclopedia of Genes and Genomes
NGS	Next-generation sequencing

References

1. Tao H, Xiong Q, Zhang F, Zhang N, Liu Y, Suo X, Li X, Yang Q, Chen M. Circular RNA profiling reveals chi_circ_0008219 function as microRNA sponges in pre-ovulatory ovarian follicles of goats (Capra hircus). *Genomics*. **2017**, *S0888-7543*, 30129-5.
2. Niu X, Huang Y, Lu H, Li S, Huang S, Ran X, Wang J. CircRNAs in Xiang pig ovaries among diestrus and estrus stages. *Porcine Health Manag*. **2022**, *8*, 29.
3. Fu Y, Zhang J, Han D, Wang HQ, Liu JB, Xiao Y, Jiang H, Gao Y, Yuan B. CiRS-187 regulates BMPR2 expression by targeting miR-187 in bovine cumulus cells treated with BMP15 and GDF9. *Theriogenology*. **2023**, *197*, 62-70.
4. Wang H, Zhang Y, Zhang J, Du X, Li Q, Pan Z. circSLC41A1 Resists Porcine Granulosa Cell Apoptosis and Follicular Atresia by Promoting SRSF1 through miR-9820-5p Sponging. *Int J Mol Sci*. **2022**, *23*, 1509.

 doi:10.20944/preprints202509.0351.v1

5. Liu Y, Wang P, Zhou Z, He X, Tao L, Jiang Y, Lan R, Hong Q, Chu M. Expression Profile Analysis to Identify Circular RNA Expression Signatures in the Prolificacy Trait of Yunshang Black Goat Pituitary in the Estrus Cycle. *Front Genet*. **2022**, *12*, 801357.
6. Wang J, Chen H, Zhang Y, Jiang S, Zeng X, Shen H. Comprehensive Analysis of Differentially Expressed CircRNAs in the Ovaries of Low- and High-Fertility Sheep. *Animals (Basel)*. **2023**, *13*, 236.
7. Lv W, An R, Li X, Zhang Z, Geri W, Xiong X, Yin S, Fu W, Liu W, Lin Y, Li J, Xiong Y. Multi-Omics Approaches Uncovered Critical mRNA-miRNA-lncRNA Networks Regulating Multiple Birth Traits in Goat Ovaries. *Int J Mol Sci*. **2024**, *25*, 12466.
8. Kechin A, Boyarskikh U, Kel A, Filipenko M. cutPrimers: A New Tool for Accurate Cutting of Primers from Reads of Targeted Next Generation Sequencing. *J Comput Biol*. **2017**, *24*, 1138-1143.
9. Kim D, Paggi JM, Park C, Bennett C, Salzberg SL. Graph-based genome alignment and genotyping with HISAT2 and HISAT-genotype. *Nat Biotechnol*. **2019**, *37*, 907-915.
10. Kim D, Langmead B, Salzberg SL. HISAT: a fast spliced aligner with low memory requirements. *Nat Methods*. **2015**, *12*, 357-360.
11. Pertea M, Kim D, Pertea GM, Leek JT, Salzberg SL. Transcript-level expression analysis of RNA-seq experiments with HISAT, StringTie and Ballgown. *Nat Protoc*. **2016**, *11*, 1650-1667.
12. Kovaka S, Zimin AV, Pertea GM, Razaghi R, Salzberg SL, Pertea M. Transcriptome assembly from long-read RNA-seq alignments with StringTie2. *Genome Biol*. **2019**, *20*, 278.
13. Pertea M, Pertea GM, Antonescu CM, Chang TC, Mendell JT, Salzberg SL. StringTie enables improved reconstruction of a transcriptome from RNA-seq reads. *Nat Biotechnol*. **2015**, *33*, 290-295.
14. Zhang XO, Dong R, Zhang Y, Zhang JL, Luo Z, Zhang J, Chen LL, Yang L. Diverse alternative back-splicing and alternative splicing landscape of circular RNAs. *Genome Res*. **2016**, *26*, 1277-1287.
15. Gao Y, Wang J, Zhao F. CIRI: an efficient and unbiased algorithm for de novo circular RNA identification. *Genome Biol*. **2015**, *16*, 4.
16. Ye J, Yao Z, Si W, Gao X, Yang C, Liu Y, Ding J, Huang W, Fang F, Zhou J. Identification and characterization of microRNAs in the pituitary of pubescent goats. *Reprod Biol Endocrinol*. **2018**, *16*, 51.
17. Cao Z, Gao D, Xu T, Zhang L, Tong X, Zhang D, Wang Y, Ning W, Qi X, Ma Y, Ji K, Yu T, Li Y, Zhang Y. Circular RNA profiling in the oocyte and cumulus cells reveals that circARMC4 is essential for porcine oocyte maturation. *Aging (Albany NY)*. **2019**, *11*, 8015-8034.
18. Liu J, Feng G, Guo C, Li Z, Liu D, Liu G, Zou X, Sun B, Guo Y, Deng M, Li Y. Identification of functional circRNAs regulating ovarian follicle development in goats. *BMC Genomics*. **2024**, *25*, 893.
19. Huang C, Feng F, Dai R, Ren W, Li X, Zhaxi T, Ma X, Wu X, Chu M, La Y, Bao P, Guo X, Pei J, Yan P, Liang C. Whole-transcriptome analysis of longissimus dorsi muscle in cattle-yaks reveals the regulatory functions of ADAMTS6 gene in myoblasts. *Int J Biol Macromol*. **2024**, *262*, 129985.
20. Li P, Wang J, Zhi L, Cai F. Linc00887 suppresses tumorigenesis of cervical cancer through regulating the miR-454-3p/ FRMD6-Hippo axis. *Cancer Cell Int*. **2021**, *21*, 33.
21. Visser-Grieve S, Hao Y, Yang X. Human homolog of Drosophila expanded, hEx, functions as a putative tumor suppressor in human cancer cell lines independently of the Hippo pathway. *Oncogene*. **2012**, *31*, 1189-1195.
22. Yang S, Wei L, Liang Q, Liu X, Li N. Research Progress on Cyclins and Cyclin-dependent Kinases Related with Primordial Follicle Activation. *Genomics and Applied Biology*. **2024**, *43*, 1321-1331.
23. Lalonde-Larue A, Boyer A, Dos Santos EC, Boerboom D, Bernard DJ, Zamberlam G. The Hippo Pathway Effectors YAP and TAZ Regulate LH Release by Pituitary Gonadotrope Cells in Mice. *Endocrinology*. **2022**, *163*, bqab238.
24. Plewes MR, Hou X, Zhang P, Liang A, Hua G, Wood JR, Cupp AS, Lv X, Wang C, Davis JS. Yes-associated protein 1 is required for proliferation and function of bovine granulosa cells in vitro†. *Biol Reprod*. **2019**, *101*, 1001-1017.
25. Ndiaye K, Castonguay A, Benoit G, Silversides DW, Lussier JG. Differential regulation of Janus kinase 3 (JAK3) in bovine preovulatory follicles and identification of JAK3 interacting proteins in granulosa cells. *J Ovarian Res*. **2016**, *9*, 71.

 doi:10.20944/preprints202509.0351.v1

26. 26. Yue J, López JM. López. Understanding MAPK Signaling Pathways in Apoptosis. *Int J Mol Sci*. **2020**, *21*, 2346.
27. Xu H, Cai Y, Yang H, Zhang C, Liu W, Zhao B, Wang F, Zhang Y. AMH regulates granulosa cell function via ESR2/ p38-MAPK signaling pathway in sheep. *Commun Biol*. **2025**, *8*, 824.
28. Zhang X, Li M, Huang M, Peng H, Song X, Chen L, Hu W, Xu W, Luo R, Han D, Shi Y, Cao Y, Li X, Hu C. Effect of RFRP-3, the mammalian ortholog of GnIH, on apoptosis and autophagy in porcine ovarian granulosa cells via the p38MAPK pathway. *Theriogenology*. **2022**, *180*, 137-145.
29. Wang J, Bai J, Liu Y, Zhang Z, Lv Z, Hai G, Li H, Liu W, Tang L, Hua Y, Wang R, Zhang Y, Fu X, Wan P. Transcriptomic characterization of lamb ovaries and oocytes reveals key biomarkers after superovulation. *J Anim Sci*. **2025**, *Jun 11*, skaf193.
30. Li G, Yan L, Wang L, Ma W, Wu H, Guan S, Yao Y, Deng S, Yang H, Zhang J, Zhang X, Wu H, He C, Ji P, Lian Z, Wu Y, Zhang L, Liu G. Ovarian overexpression of ASMT gene increases follicle numbers in transgenic sheep: Association with lipid metabolism. *Int J Biol Macromol*. **2024**, *269*, 131803.
31. Zhi F. Association Analysis of SNPs in CTNNB1 and pri-miR-458b with Laying Traits in Layers. Master's Thesis, Shandong Agricultural University, Taian, China, **2020**.
32. Liu T, Wen Y, Cui Z, Chen H, Lin J, Xu J, Chen D, Zhu Y, Yu Z, Wang C, Zhang B. MicroRNA-3061 downregulates the expression of PAX7/Wnt/Ca(2+) signalling axis genes to induce premature ovarian failure in mice. *Cell Prolif*. **2024**. *57*, e13686.
33. Du X, Li Q, Yang L, Liu L, Cao Q, Li Q. SMAD4 activates Wnt signaling pathway to inhibit granulosa cell apoptosis. *Cell Death Dis*. **2020**, *11*, 373.
34. Li K, Chen X, Dai M, Li M, Huang Y, Bai L, Wu Y, He G. The research progress of HGF/c-MET signaling pathway regulating reproductive cytogenesis. *The Journal of Practical Medicine*. **2019**, *35*, 3413-3417.
35. Xu J, Xu H, Hu L, Zhang F, Gao Q, Luo H, Zhang H, Shi R, Li X, Liu L, Guo G, Wang Y. Association Analysis of MER Gene Single Nucleotide Polymorphism with Reproduction and Milk Production on Traits in Chinese Holstein Cattle. *Acta Veterinaria et Zootechnica Sinica*. **2022**, *53*, 3769-3785.
36. Ling L, Feng X, Wei T, Wang Y, Wang Y, Wang Z, Tang D, Luo Y, Xiong Z. Human amnion-derived mesenchymal stem cell (hAD-MSC) transplantation improves ovarian function in rats with premature ovarian insufficiency (POI) at least partly through a paracrine mechanism. *Stem Cell Res Ther*. **2019**, *10*, 46.
37. Liu H, Li SR, Si Q. Retraction Note: Regulation of miRNAs on c-met protein expression in ovarian cancer and its implication. *Eur Rev Med Pharmacol Sci*. **2024**, *28*, 3891.
38. Parrott JA, Skinner MK. Developmental and hormonal regulation of hepatocyte growth factor expression and action in the bovine ovarian follicle. *Biol Reprod*. **1998**, *59*, 553-560.